Vincent Thielens, Frederiek Demeyer, Klaus Peter Geigle, Peter Kutne, Ward De Paepe
Experimental investigation of the emissions and performance of a micro gas turbine setup with enhanced EGR
Appl. Thermal Eng. 267 (2025) 12673

The original publication is available at www.elsevier.com

http://dx.doi.org/10.1016/j.applthermaleng.2025.125673

Highlights

Experimental investigation of the emissions and performance of a micro gas turbine setup with enhanced EGR

Vincent Thielens, Frederiek Demeyer, Klaus Peter Geigle, Peter Kutne, Ward De Paepe

- EGR is limited by the incompleteness of the combustion due to oxygen depletion
- An mGT is modified to control the EGR rate and operated until flame-out
- A CO_2 concentration of 7.9% is reached and 70% EGR minimizes CO emission
- EGR can increase the combustion chamber residence time promoting NO_x production
- Questions at high pressure combustion require future work at pressurized conditions

Experimental investigation of the emissions and performance of a micro gas turbine setup with enhanced EGR

Vincent Thielens[a,b,*], Frederiek Demeyer[b], Klaus Peter Geigle[c], Peter Kutne[c], Ward De Paepe[a]

[a] *Thermal Engineering and Combustion Unit, University of Mons, Rue de l'Épargne 56, Mons, 7000, Belgium*
[b] *Mechanics and Thermal Processes, Engie R&I Laborelec, Rue de Rhode 125, Linkebeek, 1630, Belgium*
[c] *Institute of Combustion Technology, German Aerospace Center, Pfaffenwaldring 38-40, Stuttgart, 70569, Germany*

Abstract

Exhaust gas recirculation (EGR) is investigated to reduce the amine-based carbon capture penalty of combined cycle gas turbines by the reduction in mass flow rate and the increase in CO_2 concentration permitted by the semi-closed cycle. Furthermore, EGR is one of the best pathways to reduce NO_x emissions. While many numerical investigations have been performed in literature, there is a clear lack of full-scale experimental investigations on a real gas turbine. To answer that need, an MTT EnerTwin® micro gas turbine has been modified and equipped with an external EGR loop allowing to apply recirculation rates up to flameout. Within the wide spectrum of EGR fraction, the composition of the exhaust gases and the combined heat

*Corresponding author
Email address: vincent.thielens@umons.ac.be (Vincent Thielens)

and power production has been measured. While EGR effectively allows to reach a dry CO_2 concentration up to 7.9%, decrease NO_x emissions and slightly improve the combined thermal and electrical production (due to the higher specific heat capacity of the working fluid, when applying EGR, and low recirculation temperature), CO emissions are the main limiting factor before flameout is reached. However, the results observed at low pressure (3-5 bar and TIT of 950 °C for mGT) cannot be directly transposed at high pressure (15-20 bar and TIT of 1300-1400 °C for industrial GT) due to the sensitivity of NO_x formation chemistry to pressure and temperature levels. The significant differences between mGTs and industrial GTs make complex any comparisons and emulations between those two scales. Extrapolating the results from mGTs to industrial GTs thus present some limitations and further investigations need to be done to understand the impact of pressure on the NO_x and CO production. Nevertheless, EGR has been characterized experimentally on a mGT and identified as a clear potential pathway to carbon neutrality by improving post combustion capture efficiency owing to the gain in CO_2 concentration.
Keywords: micro gas turbine, exhaust gas recirculation, NO_x reduction, CO emission, CO_2 concentration

Nomenclature

Acronyms	CAPEX	capital expenditure	
	CCGT	combined cycle gas turbine	
	EGR	exhaust gas recirculation	
	HHV	higher heating value	kJ/kg
	HRSG	heat recovery steam generator	
	LHV	lower heating value	kJ/kg
	mGT	micro gas turbine	
	PCC	post-combustion capture	
	TIT	turbine inlet temperature	°C
	TOT	turbine outlet temperature	°C
Greek letters	η	energy efficiency	%
	λ	air-fuel equivalence ratio	
	μ	statistical mean	
	ϕ	fuel-air equivalence ratio	
	σ	statistical standard deviation	
Roman letters	c_p	specific heat capacity	J/kg °C
	$\dot{m}$	mass flow rate	kg/s
	P	power	kW
	Q	heat duty	kW
	W	mechanical work	kW
	x	molar fraction	% mol.
Subscripts	$_{\text{amb.}}$	ambient	
	$_{\text{e}}$	electrical	
	$_{\text{th}}$	thermal	

1. Introduction

Gas turbines have already been identified as one of the pathways to carbon neutrality. On the road to zero-carbon economy, the intermittency and fluctuations of renewables need to be compensated and gas turbines come up as a flexible and efficient solution. Alongside their responsiveness to load demand, their use in combination with post-combustion capture (PCC) ensures the compliance with carbon emission levels while still valorizing the energetic and economic potential of fossil fuels.

While exhaust gas recirculation (EGR) is a well-known technique used to cut down on NO_x emissions [1], Gülen et al. [2] and De Paepe et al. [3] have also highlighted its four advantages on carbon capture as a way of:

1. increasing the CO_2 concentration;
2. decreasing the O_2 concentration (chemical stability of the amines);
3. decreasing the NO_x emissions (chemical stability of the amines);
4. decreasing the mass flow of exhaust gases to treat.

As a lower flow of exhaust gases with a higher concentration of CO_2 significantly decreases the size and the economical investments related to the carbon capture unit [4], the reduction in O_2 and NO_x concentrations also results in a benefit to the chemical stability of the amines used for after-treatment of the exhaust gases [5].

Achieving the highest level of EGR therefore seems to be a promising way of mitigating the inevitable energy penalty and CAPEX increase of post-combustion capture (PCC) by getting closer to stoichiometric conditions [4]. However, it has been shown by Ali et al. [6], Tanaka et al. [7] and El Kady et al. [1] that going below 16% of dry O_2 at the combustion chamber inlet leads to unacceptable levels of unburned hydrocarbons and CO emissions. Moreover, the implementation of EGR requires an external blower that can decrease the net power of the cycle [3].

Camaretti et al. [8] have experimented with EGR on an mGT for natural gas and biogas, and have noticed a depletion in NO_x and O_2. However, they have not applied EGR below 16% O_2 at the combustion chamber inlet. On the industrial side, Syed et al. [9] have identified the N_2O and Zeldovich's routes as the dominating mechanisms of NO_x production, however their study remains numerical. Ali et al. [6] have validated a model of mGT and have applied EGR up to 3.7% mol CO_2 in the flue gases. Nevertheless, this value remains far from the stoichiometric limit. On the numerical side, De Santis et al. [10] have investigated the impact of CO_2 on flame stabilization and flame speed in the combustion chamber of an mGT. They have shown that the increased CO_2 concentration reduces the flame speed and thus the combustion stability, nevertheless, no experimental validation has been performed. At DLR, Kutne et al. [11] have studied the flame stabilization at different pressure levels and with different EGR rates. They have highlighted that increasing the pressure allows to stabilize the flame at higher EGR rates. Even though Cameretti et al. [8], De Santis et al. [10] and Ali et al. [6] have either simulated or emulated EGR on micro gas turbines to monitor the evolution of CO, CO_2 and NO_x emissions, none of them have tried to experimentally push to the flameout limit. Furthermore, their studies have not covered the broader aspects such as the power generation or the combined production of heat. The impact of EGR on CO, CO_2, O_2 and NO_x is thus documented in literature but only for moderate recirculation rate and mostly without experimental validation.

No experiment has currently been run on a full scale gas turbine, and some works have been realized on mGT but EGR has never been applied up to the point of flameout. As a result, there is a clear need to experimentally achieve higher EGR levels and understand:

- how the power production of the machine is impacted by the EGR;
- how the quality of the heat recoverable in the economizer is impacted by the change in composition of the flue gases;
- how CO and NO_x emissions evolve while getting closer to stoichiometry;
- what is the maximal CO_2 concentration in the exhaust gases before flameout.

Those understandings are crucial to assess the impact of EGR on the power production, the combined heat recovery potential and the composition of the exhaust gases.

On the side of large-scale GTs, Tanaka et al. [7] have clearly identified the dilemma between a high combustion temperature, synonym of greater efficiency, and thermally boosted NO_x production. They have described how EGR positively decreases the emission of NO_x by cutting down on the local high flame temperature zone and enhancing the homogeneity of the air/fuel mixture. Furthermore, they have also highlighted that presence of NO_x in the air inlet, induced by EGR, has no effect on their production during the combustion. In a previous work, El Kady et al. [1] have mimicked EGR in a premixed combustor up to 1 MPa. They have shown that EGR narrows the flame stability limits but allows to reach more than 8% CO_2 on a dry basis in the flue gases. Furthermore, it has been confirmed that EGR contributes to NO_x reduction and that CO emissions are the limiting factor of EGR.

This paper thus addresses the lack of experimental studies by presenting a modified mGT where EGR rates up to flameout can be applied. This modified setup allows to investigate the impact of EGR on the exhaust mass flow rate, net power production and emissions of O_2, CO_2, NO_x and CO. In large-scale combined cycle power plant, the application of exhaust gas recirculation changes the composition of the gases flowing trough the heat recovery steam generator, potentially impacting the performances of the bottoming cycle. The presence of an external economizer in the mGT setup for the production of hot water thus enables to get some insights on the heat recovery potential in the exhaust gases. While it does not represent correctly the HRSG of a steam cycle, some trends can be extracted on how EGR impacts the quality of the heat at the turbine outlet.

By applying higher EGR rates, the experimental setup presented in this paper innovatively allows to study and understand the impacts and limits of EGR on an mGT. The heat and power production as well as the emission levels in the exhaust gases will therefore be monitored for different recirculation rate up to flameout. Given that EGR is one of the potential contributors envisaged to decarbonize CCGT, this modified setup can also be innovatively assimilated as a small-scale combined cycle gas turbine. This experimental work does not only verify the trends highlighted by the numerical simulations carried out in literature, but can also be used, under a few hypotheses, to emulate the behaviour of large-scale CCGT. Despite the significant difference between mGTs and industrial GTs, making complex any comparisons and emulations between those two scales, the approach consisting on extrapolating the results from mGT to industrial GT has been done successfully by Reboli et al. [12]. This method has however some limitations and further investigations thus need to be done to understand the impact of pressure on the NO_x and CO production.

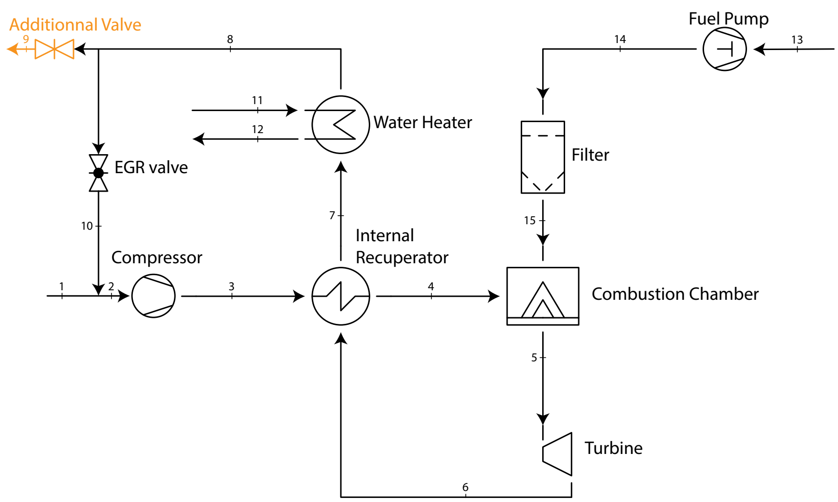

Figure 1: The MTT EnerTwin® micro gas turbine is equipped with an internal recuperator allowing to recover heat at the turbine outlet in order to preheat the air entering the combustion chamber. The experimental setup also contains a water heater for the production of warm water that can mimic an HRSG. In addition to the original EGR valve, an additional valve has been installed at the exhaust to restrict flow and force the recirculation.

2. Methodology

To fill the gaps on experimental work where EGR is applied up to flame-out, a commercial mGT has been modified and equipped with an external EGR loop as represented in Figure 1. Exhaust gas recirculation thus takes a fraction of the flue gases in the exhaust pipe (8) and recirculates them to the compressor inlet (2). By doing so, the fresh air flow rate (1), specifically the oxygen flow rate, is decreased leading to combustion conditions closer to stoichiometry.

The exhaust gas recirculation rate is defined as the ratio between the flow recirculated to the compressor (10) and the flow leaving the combustion chamber (5). While many studies are currently identifying EGR rate limitations at 40% [4] or 45% [13] leading to an air-fuel equivalence ratio λ around 1.5 (fuel-air equivalence ratio ϕ of 0.67 as shown in Figure 2) on large-scale gas turbines, the highly diluted combustion encountered in mGTs requires much larger EGR rates to reach the same equivalence ratio. Figure 3 compares the air-fuel equivalence ratio for the GE 9HA.02 and the MTT EnerTwin® for the same EGR rate. As represented in Figure 3, the air-fuel equivalence ratio of the mGT starts at 9.3 (fuel-air equivalence ratio ϕ of 0.1) when no EGR is applied. At 45% EGR, λ is still at 5.1 opposed to the 1.5 that would have been expected on an industrial GT fed with pure methane. To reach a λ of 1.5, 84% EGR needs to be applied to the mGT while the stoichiometric limit is situated at 89%. For two different turbines, the recirculation rate cannot be used to compare the operating conditions of the combustion chamber as it does not lead to the same meaning in terms of air-fuel equivalence ratio.

Starting from the operating conditions without EGR, the exhaust gases are progressively recirculated while keeping constant the mass flow in the combustion chamber. A simple input-output modelled is used assuming complete combustion of fuel. The dry and wet compositions of the gases before and after the combustion chamber are then computed. It can be observed in Figure 4 that 71% EGR are required to move the dry O_2 fraction from 21% (air related with no EGR) towards the 16% dry limit announced by El-Kady

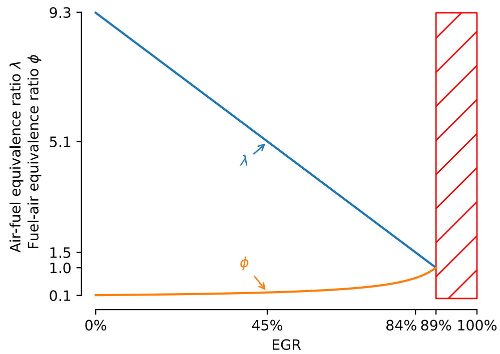

Figure 2: Starting at 9.3, the air-fuel equivalence ratio λ decreases linearly with the EGR level to reach 1 at stoichiometry when 89% of EGR is applied. Due to the high dilution rate, 84% of EGR has to be applied to reach a λ of 1.5, equivalent to the value encountered with 45% EGR on a large-scale industrial gas turbine.

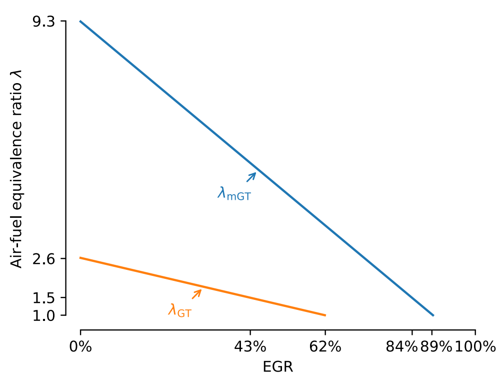

Figure 3: Compared to the GE 9HA.02, the higher dilution encountered in a micro gas turbine allows to apply a bigger recirculation rate for a same λ. For instance, the stoichiometry is reached with a recirculation rate of 62% for an industrial GT, this is only obtained with 89% of recirculation rate for the mGT.

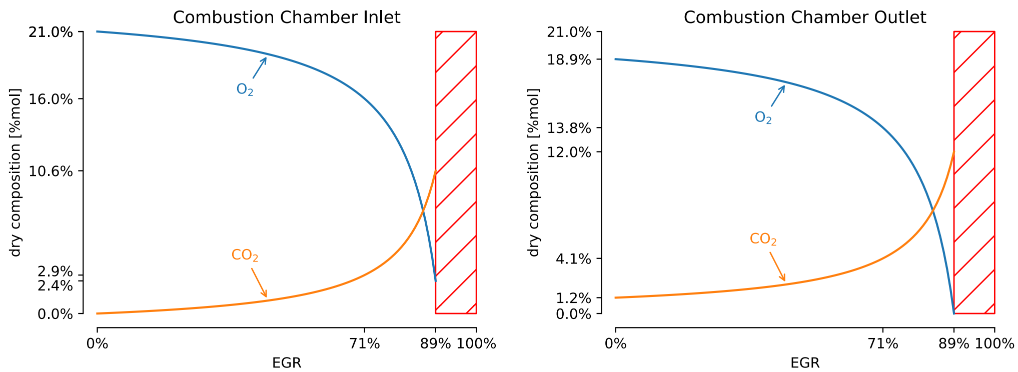

Figure 4: The application of EGR allows to increase the CO_2 concentration at the combustion chamber inlet and outlet as well as decreasing the O_2 molar fraction. The maximum EGR level that can be applied to keep analytically a complete combustion is 89%. At 71% of EGR, the O_2-concentration at the combustor inlet reaches 16%.

et al. [1]. At that level, the exhaust gas contains 4.1% of CO_2 and 13.8% of O_2 on a dry molar basis. Nevertheless, Figure 4 shows that higher recirculation rates can be theoretically expected to reach the stoichiometric limit at 89% EGR. That limit therefore maximises the CO_2 outlet concentration (12%) but also leads to the most severe combustion condition with only 2.4% of O_2 at the combustion chamber inlet. Those conditions are difficult to stabilize in real combustion chambers and the emissions of CO and unburned are often limiting factors, lowering the achievable EGR rate.

While the analytical equilibrium-based laws allow to predict the dry molar composition of the exhaust gases, at both the inlet and outlet of the combustion chamber, some questions are remaining with respect to:

- kinetic mechanisms related to the production of NO and NO_2;

- incomplete combustion leading to the production of CO;
- flexibility of the combustor to come closer to the stoichiometric limit.

An experimental setup where higher EGR rates can be applied is therefore required to observe the evolution of:

- the concentration of CO_2;
- the concentration of O_2;
- the concentration of CO;
- the concentration of NO and NO_2;
- the net electrical power produced;
- the heat recovered from the exhaust gases for cogeneration via hot water production.

2.1. Initial unmodified setup

The initial setup is an MTT EnerTwin® micro gas turbine which can produce between 1.0 and 3.2 kW_e combined with a thermal production ranging from 6.0 to 15.6 kW_{th}. Alongside electricity generation, this mGT has the option to produce domestic hot water (up to 80 °C). While the net grid output efficiency varies between 10 and 16%, the combination with the heating system allows to achieve a total efficiency exceeding 94% of the LHV.

As represented in Figure 1, the MTT EnerTwin® mGT exploits the recuperated Brayton cycle. The inlet air enters the variable speed radial compressor (2) at atmospheric conditions and is compressed up to 2.4 bar. After the compression (3), the air is preheated in the internal recuperator up to 720 °C (4), where it encounters a pressure drop, before being mixed with natural gas in the combustion chamber. The flow (5) is then expanded through the turbine to 1 bar (6) and a fraction of the remaining energy is transferred to the compressed air in the internal recuperator by cooling the exhaust gases from 790 °C down to 230 °C (7). The flow finally enters the water heater for the combined heat purpose where in the setup tap water is employed as cooling agent. This uncommon practice allows the exhaust gases to be cooled as low as 14 °C (8).

The manufacturer has already foreseen an EGR valve in the mGT allowing a fraction of the exhaust gases to be recirculated to the compressor inlet (10). While working with higher exhaust gas temperatures (related to a production of hot water when a buffer is connected to the mGT), the control logic monitors the EGR valve opening to decrease the electric power production when the grid inverter current limit is reached. Alongside the electric current limit, the inner controller allows to enter different set-points in order to regulate the thermal power. The control algorithm will then monitor the fuel pump and the rotational speed so that the turbine outlet temperature (6) remains constant.

The mGT has been equipped with different sensors allowing to measure the temperature, pressure and flow rate at different locations. The composition of the flue gases is measured with a Testo® 350 analysis box that can survey the evolution of O_2, NO, NO_2, CO and CO_2 with an infrared cell. The uncertainties related to the measurement of the exhaust gases are presented in Table 1. The pressure levels are measured with Huba Control® sensors (absolute error ±0.012 bar) and temperatures either with Tasseron® NTC 10K3% sensors (absolute error ±0.9 °C) or with K-type thermocouples (absolute error ±2.2 °C). The inlet air mass flow is measured with the vortex flowmeter from Yokogawa® and the gas flow with the Elster® BK-G4M16 (absolute error ±2% of read value).

2.2. Manual control of the EGR valve

Although the EGR valve was already controlled by the inner controller of the mGT, the EGR level needs to be changed independently from the control system. The connection lines to the valve have therefore been cut and linked to an external control system allowing to manually decide the closing of the valve. The designed PID system enhances to vary the closing ratio from 0 to 100% at the proper moment imposed by the testing campaign. The PID has been implemented on an Arduino Uno® board and gives a signal to the L298 full-bridge driver, controlling the DC motor, based on the closing angle

component	measuring range	accuracy	resolution	reaction time t_{90}
O_2	0 - 25 % vol.	± 0.8% of fsv	0.01 % vol.	20 s
CO	0 - 199 ppm	± 10 ppm	1 ppm	40 s
	200 - 2 000 ppm	± 5% of mv	1 ppm	40 s
	2 001 - 10 000 ppm	± 10% of mv	1 ppm	40 s
NO	0 - 99 ppm	± 5 ppm	1 ppm	30 s
	100 - 1 999 ppm	± 5% of mv	1 ppm	30 s
	2 000 - 4 000 ppm	± 10% of mv	1 ppm	30 s
NO_2	0 - 99.9 ppm	± 5 ppm	0.1 ppm	40 s
	100 - 500 ppm	± 5%	0.1 ppm	40 s
CO_2	0 - 25% vol.	± 0.3% vol. + 1% of mv	0.01% vol.	10 s
	25 - 50% vol.	± 0.5% vol. + 1.5% of mv	0.1% vol.	10 s

Table 1: Testo® refers for each cell the measuring range, the accuracy, the resolution as well as the reaction time t_{90}. (mv: measured value, fsv: full-scale value)

of the valve measured with a KMA210 angle sensor.

When fully open, the EGR valve only allows to recirculate up to 30% of the flue gases. As indicated in Figure 2, this is too low to reach flameout. On large-scale CCGTs, EGR levels can reach 45% in an adapted combustor before combustion issues are faced (e.g. incomplete combustion) due the air-fuel ratio close to stoichiometry. However, the highly diluted combustion encountered in mGTs ($\lambda \simeq 9.4$) requires much larger EGR levels to reach the same richness as the one in the industrial combustors. In order to exceed the limit of 30% EGR, still leading to a highly diluted combustion ($\lambda \simeq 6.6$), an additional valve has been placed in the exhaust gas duct as represented in orange in Figure 1. This valve increases the pressure drop in the exhaust pipe (9) and forces a higher fraction of the flow to be recirculated (10) (throttling effect). This last modification leads to recirculation ratios reaching 84% and combustion conditions closer to stoichiometry. As the combustion issues are faced for a λ around 1.5 in industrial GTs, it is interesting to investigate the stability of the combustor as well as the emission levels for this richness. Moreover, a given closing angle of the exhaust valve leads to the flame being extinguished, and therefore makes it possible to test all the EGR levels physically achievable on this installation. As explained by Pappa et al. [14], the flameout is related to the staggering of the combustion chamber where the primary zone encounters smaller equivalence ratio λ (between 0.29 and 0.44), while the overall equivalence ratio is equal to 1.5.

2.3. Experimenting with natural gas

The fuel price can be a real constraint restricting the number of experiments as well as their duration. While working with pure methane reduces the uncertainties related to the fuel gas composition and thus to the computation of the exhaust gas composition, its price per kWh can be 30 up to 60 times more expensive than working with natural gas. However, natural gas has the main drawback of an unknown mean composition that is changing daily.

According to the data delivered by the gas provider, the natural gas delivered in the UMONS lab is composed of: CH_4, C_2H_6, C_3H_8, C_4H_{10}, C_5H_{12}, He, N_2, CO_2 as well as higher refined gases (C_6H_{14} and more). For simplicity reasons in the chemical equations, natural gas is written under its summarized formula: $C_xH_yN_zO_v$.

For each fuel, the maximal amount of CO_2 in the exhaust gases is obtained at stoichiometry as presented in Equation 1 for the molar ratio of air S^* computed in Equation 2. The dry maximal molar concentration $CO_{2,\,\mathrm{max}}$, that will be used afterwards, can be directly deduced from the fuel composition as expressed in Equation 3. Based on the data provided by the gas provider, the $CO_{2,\,\mathrm{max}}$ is computed and represented in Figure 5. While methane has a $CO_{2,\,\mathrm{max}}$ of 11.7%, the presence of gases with longer carbon chains in natural gas leads to an expected value slightly higher than 12.05%. Besides its lower cost, experimenting with natural gas allows thus to reach higher CO_2 content in exhaust gases and facilitates to simulate situations with a lower level of oxygen at the combustion chamber inlet.

$$\begin{aligned} \mathrm{C}_x\mathrm{H}_y\mathrm{N}_z\mathrm{O}_v + S(0.21\mathrm{O}_2 + 0.79\mathrm{N}_2) \rightarrow & x\mathrm{CO}_2 + \frac{y}{2}\mathrm{H}_2\mathrm{O} + \left(\frac{z}{2} + 0.79S\right)\mathrm{N}_2 \\ & + \left(\frac{v}{2} + 0.21S - x - \frac{y}{4}\right)\mathrm{O}_2 \text{ [15]} \end{aligned} \quad (1)$$

$$\frac{v}{2} + 0.21S^* - x - \frac{y}{4} = 0 \leftrightarrow S^* = \frac{x + \frac{y}{4} - \frac{v}{2}}{0.21} \text{ [15]} \quad (2)$$

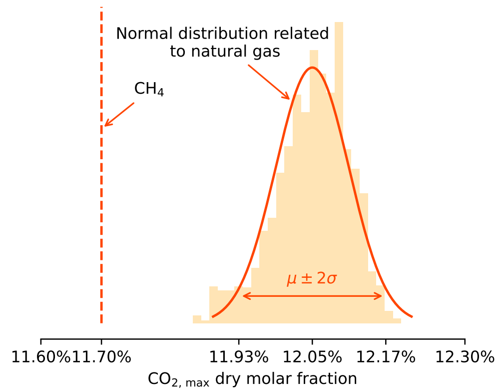

Figure 5: 95% of the maximal CO_2 dry molar fraction, resulting from the stoichiometric combustion of natural gas, is located between 11.93% and 12.17%. Due to the presence of atoms with a higher carbon content in natural gas, the $CO_{2,\ \mathrm{max}}$ of methane (11.7%) is below the one of natural gas (12.05%).

$$\mathrm{CO}_{2,\ \mathrm{max}} = \frac{x}{x + \left(\frac{z}{2} + 0.79S^*\right)} = \frac{x}{x + \left(\frac{z}{2} + 0.79\frac{x + \frac{y}{4} - \frac{v}{2}}{0.21}\right)} \ [15] \tag{3}$$

2.4. Organization of the testing campaign

To carry out the tests, the mGT was first preheated for two hours at a set point of 70%. The preheating phase heats up the components (in particular the heat exchangers and combustion chamber) so that their temperatures are constant. Ten different EGR rates are then applied, waiting up to 30 minutes between each to ensure that stability is achieved. During the post-treatment phase, the data is averaged over the last 5 minutes of the applied EGR rate.

3. Results and discussion

The experimental setup previously presented is run on a range of EGR ratios starting from 0% up to flameout at 84%. The power produced and the heat transmitted to the water are then measured and the composition of the exhaust gas is analysed in terms of O_2, CO_2, NO_x and CO.

3.1. Global cycle performance

The impact of EGR on the net power and the heat duty have been computed and are represented in Figure 6. Measurements at the generator terminals show that EGR positively affects the electrical production. Indeed, the net power produced increases by 2.1 W_e per additional EGR percentage and applying 80% EGR thus leads to a relative increase of 8%. This tendency is explained by:

- the control strategy of the mGT keeping a constant TOT;
- the below-ambient temperature of the recirculated gases (due to indirect tap water cooling).

At the outlet of the water heater (point 8 in Figure 1), the exhaust gases are cooled down to around 14 °C. This temperature is 5 °C lower than the ambient temperature and applying EGR therefore decreases the compressor inlet temperature (2) proportionally. While a colder flow (2) at the compressor inlet is beneficial to the cycle, this also means that the compressor outlet temperature (3) is decreased and subsequently the combustion chamber inlet temperature (4) too. Although this phenomenon is partially counteracted by the recuperator, more fuel is consumed to maintain a constant TOT, allowing more heat to be recovered from the water heater, as can be seen in Figure 6. Per percentage of EGR applied, an additional 24 W_{th} is recovered in the water heater and this represents a 14% increase at 80% EGR. As opposed to the simulations presented by De Paepe et al. [3], the absence of auxiliaries and the lower air inlet temperature of this setup benefit to the cycle. The mGT installed in the UMONS lab does not suffer from high back pressure when advanced recirculation rates are applied. This result is obtained thanks to the added external recirculation loop which have a diameter high enough to allow recirculation without significant friction loss. It is the combined effect of the large diameter with the relative small flow rate. An external fan is therefore not needed and the back pressure only increases by 600 Pa between 0% EGR and 84% EGR.

Furthermore, the last author of this paper has raised in previous work [3] the question of the impact of the change in composition on the cycle performance. To get rid of the impact of the recirculated gases colder temperature, new experiments have been realized when the ambient temperature (1) is equal to the recirculation temperature at the outlet of the water heater (8). When the compressor inlet (2) temperature is maintained at 16 °C, one can see that EGR still increases the net power and the heat duty of the cycle (Figure 8). However, the slopes of the dashed regression lines from Figure 6

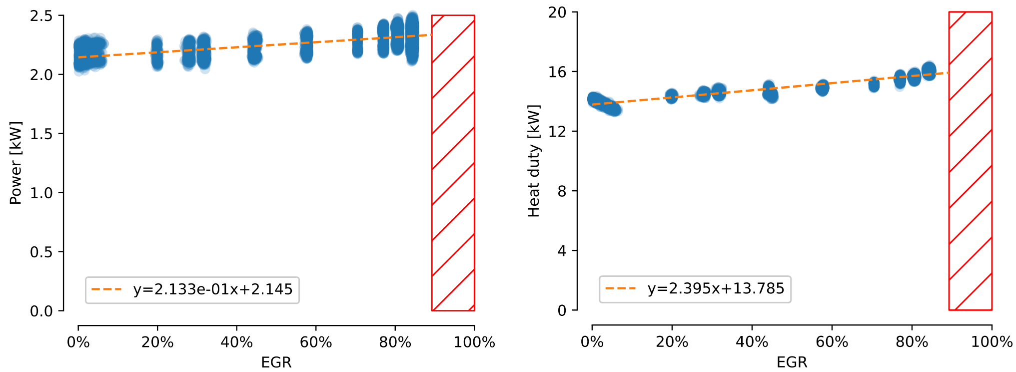

Figure 6: The application of EGR increases the net power production as well as the heat recovery potential in the conditions where the temperature of the recirculated gases (14 °C) is lower than the ambient temperature (16 °C).

are reduced in Figure 8 respectively with 36% and 33%, leading to more constant heat and power productions. This phenomenon is explained by the change in composition of the flue gases. Indeed, EGR increases the content of water in the flow leading to a higher c_p. From 1030 J/kg °C when no EGR is applied, the c_p reaches 1141 J/kg °C at the turbine inlet when 84% of the exhaust gases are recirculated (Figure 7). At the compressor side, the c_p changes from 1003 J/kg °C to 1119 J/kg °C. In order to keep a constant TOT, more fuel is thus required and the combined heat and power productions are increased.

The evolution of the net work W_{net} is described by Equation 4 where the fluid properties show to have a significant impact (γ and c_p). As previously explained, the EGR rate changes the composition of the gases flowing trough the turbomachinery Figure 7. Based on the variation in c_p and γ depicted

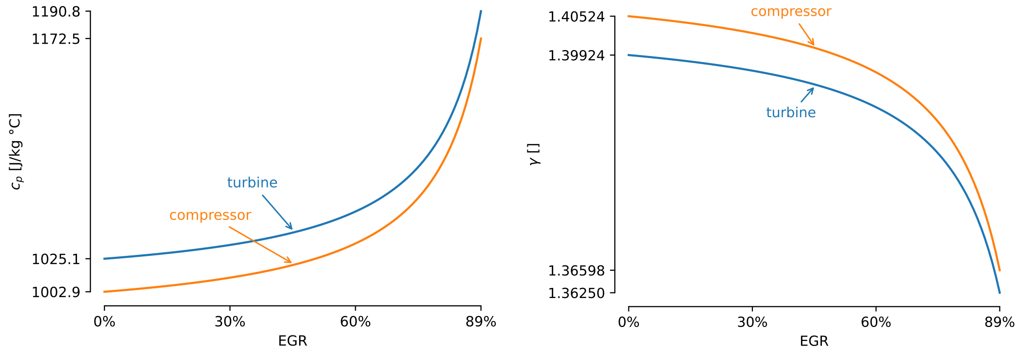

Figure 7: Due to the composition change and the higher H_2O content, the c_p increases with the application of EGR, however the heat capacity ratio γ decreases.

in Figure 7, the relative increase in net work $W_{\text{net, x\% EGR}}/W_{\text{net, 0\% EGR}}$ can be analytically computed as depicted in Figure 9. While the experimental work highlighted a relative increase of 1.13 Figure 8 at the maximal allowable level of EGR, regarding the stability of combustion, the following analytical expression predicts a relative increase of 1.11 Figure 9. The small difference between those two values comes from the simplified model presented in Equation 4 in terms of the evolution of turbomachinery efficiency and fluid properties. As demonstrated in Figure 8, the back pressure increase does not have a strong impact on the net power production. The 600 Pa maximal raise in the back pressure is indeed not sufficient to invert the trend in the enhancement of the power production due to change in fluid properties.

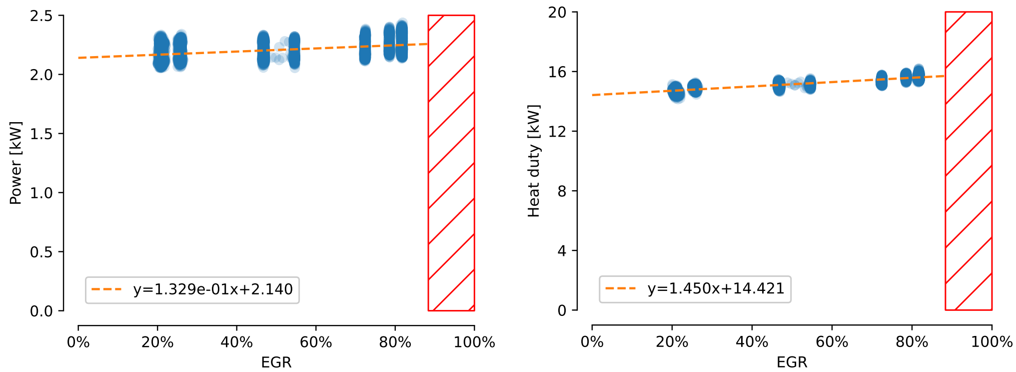

Figure 8: The application of EGR, when the compressor inlet temperature is maintained constant increases more slightly the net power production and the heat recovery potential.

$$W_{\text{net}} = -\left(W_c + W_t\right) = -\dot{m}\left(\frac{c_{p,2}}{\eta_c}T_2\left(\left(\frac{p_3}{p_2}\right)^{\dfrac{\gamma_2 - 1}{\gamma_2}} - 1\right) + c_{p,5}\eta_t T_5\left(\left(\frac{p_6}{p_5}\right)^{\dfrac{\gamma_5 - 1}{\gamma_5}} - 1\right)\right) \quad [16] \tag{4}$$

For this latter experiment, the efficiency Equation 5 is computed based on the higher heating value (HHV) to take into account the partial condensation occurring in the water heater (7-8) Figure 1. Figure 10 shows that EGR slightly increases the efficiency η_{HHV}. This evolution is due to the increase in W_{e} and Q_{th} related to the higher specific heat capacity encountered when partial recirculation is applied. Regarding to the net work W_{e}, the evolution of the composition during the different EGR levels increases the net power as described by Equation 4 represented in Figure 9. Regarding the heat flux Q_{th}, the increase of the mass heat capacity has a positive impact on the external economizer. Indeed, the control strategy ensuring a constant TOT makes

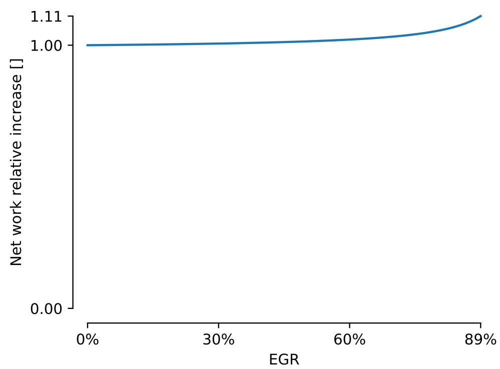

Figure 9: The evolution of the relative work when the variations in c_p and γ are taken into account, as calculated in the analytical Equation 4, shows that a relative increase of 11% is reached when 89% of EGR is applied.

the economizer hot inlet temperature constant, while the high efficiency of the economizer also enables a constant hot outlet temperature among the different EGR levels. As the temperature difference remains constant, the increase in c_p directly leads to a higher heat recovery.

$$\eta_{\mathrm{HHV}} = \frac{P_{\mathrm{e}} + Q_{\mathrm{th}}}{\dot{m}_{\mathrm{fuel}}\mathrm{HHV}} \text{ [16]} \tag{5}$$

3.2. O_2, CO_2, NO_x and CO content

Figure 11 shows that the O_2 dry fraction follows the analytical predictions presented in Figure 4. Starting at 18.9%, when no EGR is applied due to the highly diluted conditions, the concentration of O_2 in the exhaust gas reaches a minimum at 6.6% with 84% of EGR.

Figure 12 shows that the CO_2 dry fraction, measured with the infrared cell, follows the analytical predictions presented in Figure 4. Starting at 1.2%

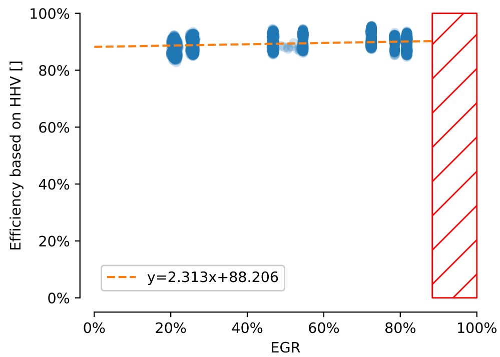

Figure 10: The efficiency slightly increases with the EGR rate has highlighted by the positive slope of the regression line (0.02% per additional EGR percentage).

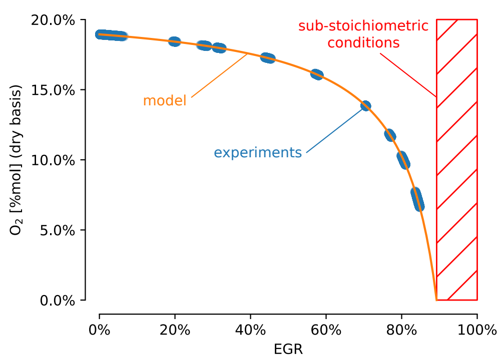

Figure 11: The dry molar composition of O_2 at the combustion chamber outlet follows the theoretical curves when EGR is applied.

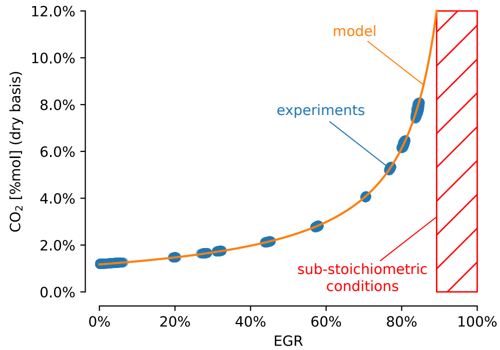

Figure 12: With the EGR level, the combustion conditions come closer to stoichiometry and the dry molar composition of CO_2 increases. The measurements in the exhaust gases (blue dots) follows the theoretical predictions (orange line). However, the recirculation rate cannot exceed 84%, as the mixture would be too rich, leading to flameout.

CO_2 content when no EGR is applied, the exhaust gases composition evolves to a maximum of 7.9% with 84% of EGR. Afterwards, additional recirculation leads to a flameout making higher CO_2 concentrations unachievable.

Due to the combustor architecture [17], a part of the incoming air is separated from the main air and passes through dilution holes. A fraction of the O_2 entering the combustion chamber is thus not usable for the combustion explaining the limitation to a λ of 1.5. The ratio between the air entering the primary zone and the total incoming air has been estimated between 20% and 30%. The equivalence ratio λ in the primary zone is therefore between 0.29 and 0.44, when the overall equivalence ratio is equal to 1.5.

The concentration of NO and NO_2 are measured in the exhaust duct by means of the Testo® 350 gas analyser. It can be observed in Figure 13 that EGR impacts the NO_x concentrations as well as their emissions by also reducing the mass flow rate of exhaust gases. Due to the combustion chamber temperature (more than 1000 °C), thermal NO is produced according to Zeldovich's mechanism, however the low residence time encountered does not favour the conversion of NO into NO_2. As expected, NO_2 is less present in the exhaust gases (approx. 2 ppm) than NO (between 10 and 20 ppm).

Up to 50% EGR, the concentration of NO is increasing due to the fictive additional residence time provided by EGR. Whereas the flow rate through the combustion chamber remains constant, EGR decreases the flow rate of fresh air by applying internal recirculation. In addition to the recirculated NO_x, additional NO_x is added by the Zeldovich's mechanism during combustion increasing their concentration in the exhaust gases. Beyond 50% EGR, the depletion in oxygen and nitrogen decreases NO_x formation.

When the reduction of exhaust flow is taken into account, EGR clearly appears as an advantageous way of cutting NO_x emissions as represented in Figure 13. While the concentration of NO_x slightly increases up to 50% EGR, the decrease in mass flow rate leads to lower total emissions.

Moreover, the reduction of oxygen in the flue gases benefits to the level of $NO_x|_{15\%\ O_2}$. Indeed, as presented in Equation 6, the presence of the molar fraction of O_2 (x_{O_2}) at the denominator further decreases the NO_x concen-

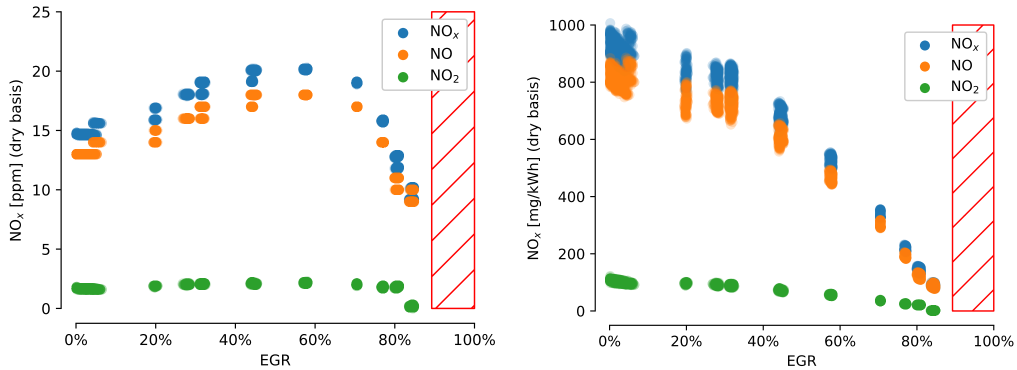

Figure 13: Due to the low residence time, NO_2 is less present in the exhaust gases than NO, however a maximum in NO concentration is encountered at around 50% EGR. Nevertheless, the decrease in mass flow rate leads to lower total emissions.

tration restored at 15% O_2 as presented in Figure 14.

$$\mathrm{NO}_x|_{15\%\ \mathrm{O}_2} = \mathrm{NO}_x|_{\mathrm{dry}} \left(\frac{\mathrm{O}_{2,\ \mathrm{amb.}}\% - 15\%}{\mathrm{O}_{2,\ \mathrm{amb.}}\% - x_{\mathrm{O}_2}\%} \right) \tag{6}$$

Due to mixing issues, a lack of O_2 is partially encountered in the chamber leading to incomplete combustion and production of CO. Up to 70% EGR, the CO concentration in the exhaust gases remains under 300 ppm. On that range, it can be observed in Figure 15 that the concentration increases slightly by reaching a plateau level at 70% EGR (± 32 ppm) roughly two times the value measured when no EGR is applied (± 16 ppm). From an EGR rate of 70%, the CO concentration evolves exponentially with higher EGR rate, rising up to 2700 ppm at 84%. The combustion architecture is composed of a primary zone in which enters roughly 30% of the incoming air. While the overall air equivalence ratio λ is still around 3.3 when 64% EGR

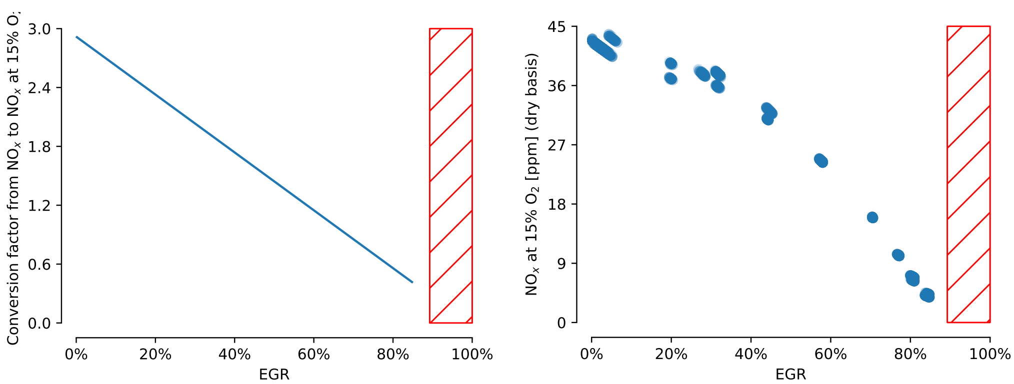

Figure 14: Environmental legislations often refer to NO_x emission referenced to 15% dry O_2. Above 64% EGR, the conversion factor from NO_x to $NO_x|_{15\%\ O_2}$ is lower than one, the application of EGR thus benefits to the NO_x reduction from a legislative point of view.

are applied, the stoichiometry is reached in the primary zone. The application of higher EGR rates therefore results in increased CO production, which is only partially burnt in the secondary zone due to the low temperature of the incoming air.

In addition to the lack of oxygen, the main cause of CO production, the dissociation of CO_2 has also been identified as a contributing factor to CO emissions [1]. The CO_2 present in the inlet composition thus also reacts through different mechanisms described by Masri et al. [18] in Equation 7, Equation 8, Equation 9 and Equation 10 to form CO. In Equation 9, M refers to a molecular third-body enhancing the efficiency of the reaction ($M = H_2O$, CO_2, H_2, CO, O_2 or N_2).

$$CO + OH \leftrightharpoons CO_2 + H \text{ [18]} \tag{7}$$

$$CO + HO_2 \leftrightharpoons CO_2 + OH \text{ [18]} \tag{8}$$

$$CO + O + M \leftrightharpoons CO_2 + M \text{ [18]} \tag{9}$$

$$CO + O_2 \leftrightharpoons CO_2 + O \text{ [18]} \tag{10}$$

However, the application of EGR decreases the exhaust mass flow rate and positively impacts the specific CO production (mg/kWh). As shown in Figure 15, the amount of specific CO emitted decreases with EGR and reaches a minimum at 70%, corresponding to 16% O_2 at the combustion chamber inlet. This first tendency is explained by the slight increase of the concentration in the exhaust gases counteracted by the exhaust flow decrease. After 70% EGR, the specific CO emission increases due to the exponential growth of its concentration. CO thus appears as a limiting factor for EGR.

4. Future work

The realized experiments have shown that EGR has the potential to increase the CO_2 concentration and decrease the mass flow of flue gases while keeping good performance. However, particular attention has to be made on the CO emissions to ensure that the legal limits are respected. While the results obtained already answer open questions from literature by experimen-

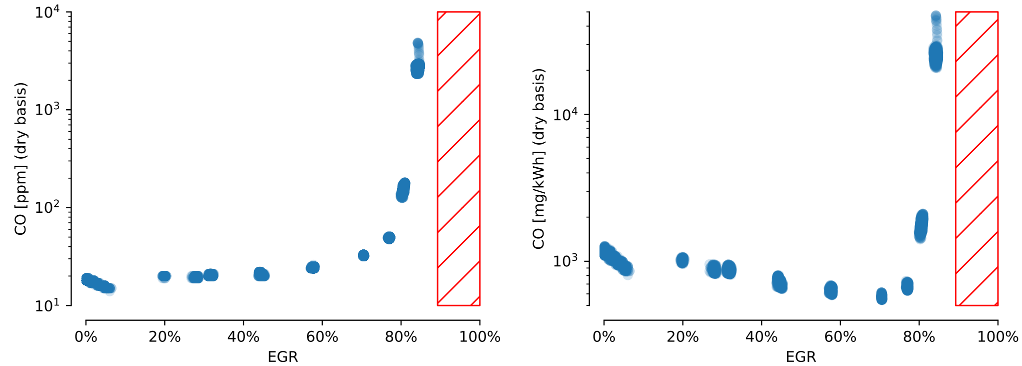

Figure 15: While EGR increases the specific CO concentration in the exhaust gases, a minimum in the CO emission is encountered at 70%, corresponding to the 16% dry O_2 at the combustor inlet.

tal evidence, further work should be planed to better understand the impact and limitations of exhaust gas recirculation.

Regarding the pressure levels, the combustor pressure is limited at 2.4 bar which is far from the range (15-30 bar) reached on an industrial gas turbine. Experiments at high pressure will therefore allow to better understand the influence of the pressure on CO and NO_x emissions when different rates of EGR are applied.

Tanaka et al. [7] have shown that the NO_x contained in the air have no effect on additional formation during the combustion. Nevertheless, EGR significantly increases the amount of NO_x at the combustion chamber inlet. Deeper investigations should be done to observe how NO_x are subject to the additional fictive residence time of EGR, to the O_2 depletion and CO_2

increase as well as by the reburning phenomenon [19]. In this phenomenon, NO is intermediately converted in HCN before being converted back to N_2.

On the CO side, further analysis on the CO reburning phenomenon should be realized to focus on how EGR can reduce CO by recirculating a fraction on the incomplete products present in the exhaust gases through the combustion chamber.

While EGR was so far applied in steady-state, no experiment has yet tried a cold-start with the direct application of EGR. Some comparisons could then be done on the emission levels and performances achieved when different levels of EGR are directly applied at the cold start of the turbine. Furthermore, transient aspects related to the recirculation of the exhaust gases have also never been investigated.

5. Conclusions

The benefits of EGR have clearly been identified on both NO_x reduction aspects, as well as for the carbon capture perspective due to the increase in concentration of CO_2, the O_2 depletion and the mass flow reduction. However, the main limiting factors of EGR are the combustion instabilities and the CO produced. While the numerical impact of EGR on the performance of the mGT has been simulated in some papers, a clear lack of experimental investigations was present.

In this paper, an innovative setup is presented where the MTT EnerTwin® has been modified with an external EGR loop recirculating gases up to flameout. The experimental setup is a micro gas turbine designed for combined heat and power generation purposes and fed with natural gas.

At the maximum EGR level (84%), the dry CO_2 concentration in the exhaust gases reached 7.9%. Over the entire recirculation spectrum, CO_2 concentration increased according to the analytical expression. While the NO_x concentration reaches a maximum of 20 ppm at around 50% EGR (due to the fictive higher residence time), the specific emission (mg/kWh) keeps decreasing with EGR due to a reduced total flue gas flow rate. On the CO side, its constant augmentation in concentration is counteracted by the reduction of the mass flow rate up to 70% EGR, after which its emissions rise sharply. Regarding the combined heat and power production, the application of recirculation, with a lower than ambient recirculation temperature increases both the power production and the heat recovered in the water heater. This tendency can be explained by the higher mass heat capacity of the flue gases and the control strategy ensuring a constant TOT, resulting in a higher heat duty.

While the realized experiments address the need of experimental data on the cycle performance when EGR is applied, some questions remain unanswered regarding to the NO_x and CO production at high pressure as well as their reburning in the combustion chamber. These considerations will be the subject of future work.

Even if the results of EGR observed on an mGT (i.e. the higher CO_2 content and lower exhaust mass flow rate) have not yet be extrapolated to an industrial size, the application of EGR already appears as a clear pathway to reduce the penalty of amine-based carbon capture unit. However, CO has already been identified as the main limiting factor to higher recirculation rate, requiring further development in combustor technologies.

6. Acknowledgments

This research is funded by the Belgian Fund for Scientific Research (F.R.S.-FNRS). Vincent THIELENS is a Research Fellow of the Fonds de la Recherche Scientifique - FNRS. This work was supported by the Fonds de la Recherche Scientifique – FNRS under Grant No J.0033.23 ACCURATE.

7. Declaration of interests

The authors declare that they have no known competing financial interests or personal relationships that could have appeared to influence the work reported in this paper.

8. Declaration of Generative AI and AI-assisted technologies in the writing process

During the preparation of this work the author(s) used chatGPT 4o in order to improve readability and language of the text. After using this tool/service, the author(s) reviewed and edited the content as needed and take(s) full responsibility for the content of the publication.

References

[1] A. M. ElKady, A. Evulet, A. Brand, T. P. Ursin, A. Lynghjem, Application of Exhaust Gas Recirculation in a DLN F-Class Combustion System for Postcombustion Carbon Capture, Journal of Engineering for Gas Turbines and Power 131 (2009) 034505.

[2] S. C. Gülen, C. Hall, Gas Turbine Combined Cycle Optimized for Post-Combustion Carbon Capture, Vol. Volume 3: Coal, Biomass and Alternative Fuels; Cycle Innovations; Electric Power; Industrial and Cogeneration Applications; Organic Rankine Cycle Power Systems of Turbo Expo: Power for Land, Sea, and Air, 2017, p. V003T08A008.

[3] W. De Paepe, M. Montero Carrero, S. Giorgetti, A. Parente, S. Bram, F. Contino, Exhaust gas recirculation on humidified flexible micro gas turbines for carbon capture applications, in: Turbo Expo: Power for Land, Sea, and Air, Vol. 49743, American Society of Mechanical Engineers, 2016, p. V003T06A011.

[4] A. Verhaeghe, M. J. Mendoza Morales, J. Blondeau, F. Demeyer, L. Bricteux, W. De Paepe, Thermodynamic Assessment of a Combined Cycle Gas Turbine With Exhaust Gas Recirculation Under Part-Load Operation Toward Carbon Capture Penalty Reduction, in: Turbo Expo: Power for Land, Sea, and Air, Vol. 86984, American Society of Mechanical Engineers, 2023, p. V005T06A008.

[5] B. Fostås, A. Gangstad, B. Nenseter, S. Pedersen, M. Sjøvoll, A. L. Sørensen, Effects of NOx in the flue gas degradation of MEA, Energy Procedia 4 (2011) 1566–1573.

[6] U. Ali, T. Best, K. N. Finney, C. F. Palma, K. J. Hughes, D. B. Ingham, M. Pourkashanian, Process Simulation and Thermodynamic Analysis of a Micro Turbine with Post-combustion CO2 Capture and Exhaust Gas Recirculation, Energy Procedia 63 (2014) 986–996, 12th International Conference on Greenhouse Gas Control Technologies, GHGT-12.

[7] Y. Tanaka, M. Nose, M. Nakao, K. Saitoh, E. Ito, K. Tsukagoshi, Development of low NOx combustion system with EGR for 1700 C-class gas turbine, Mitsubishi Heavy Industries Technical Review 50 (2013) 1–6.

[8] M. C. Cameretti, R. Tuccillo, R. Piazzesi, Study of an exhaust gas recirculation equipped micro gas turbine supplied with bio-fuels, Applied Thermal Engineering 59 (2013) 162–173.

[9] K. J. Syed, E. Buchanan, The nature of nox formation within an indus-

trial gas turbine dry low emission combustor, in: Turbo Expo: Power for Land, Sea, and Air, Vol. 4725, 2005, pp. 11–18.

[10] A. De Santis, D. B. Ingham, L. Ma, M. Pourkashanian, CFD analysis of exhaust gas recirculation in a micro gas turbine combustor for CO2 capture, Fuel 173 (2016) 146–154.

[11] P. Kutne, J. Richter, J. D. Gounder, C. Naumann, W. Meier, Exhaust Gas Recirculation at Elevated Pressure Using a FLOX® Combustor, in: Turbo Expo: Power for Land, Sea, and Air, Vol. 50848, American Society of Mechanical Engineers, 2017, p. V04AT04A078.

[12] T. Reboli, M. Ferrando, L. Mantelli, L. Gini, A. Sorce, J. Garcia, R. Guedez, Gas turbine combined cycle range enhancer-part 1: Cyber-physical setup, in: Turbo Expo: Power for Land, Sea, and Air, Vol. 86014, American Society of Mechanical Engineers, 2022, p. V004T06A022.

[13] Z. Liu, I. A. Karimi, New operating strategy for a combined cycle gas turbine power plant, Energy Conversion and Management 171 (2018) 1675–1684.

[14] A. Pappa, F. F. Nicolosi, A. Verhaeghe, L. Bricteux, M. Renzi, W. De Paepe, Performance and emission assessment on a 3kw micro gas turbine: comparison of rans and les predictions, in: Turbo Expo:

Power for Land, Sea, and Air, Vol. 84997, American Society of Mechanical Engineers, 2021, p. V006T19A015.

[15] C. Baukal, The John Zink Hamworthy Combustion Handbook: Volume 1 - Fundamentals, Industrial Combustion, CRC Press, 2012.

[16] S. L. Dixon, C. Hall, Fluid mechanics and thermodynamics of turbomachinery, Butterworth-Heinemann, 2013.

[17] D. Cirigliano, F. Grimm, P. Kutne, M. Aigner, Oxidation-Induced Damage Modeling in Micro Gas-Turbine Combustion Chambers, Procedia Structural Integrity 42 (2022) 1728–1735.

[18] A. Masri, R. Dibble, R. Barlow, Chemical kinetic effects in nonpremixed flames of H2/CO2 fuel, Combustion and Flame 91 (1992) 285–309.

[19] L. Smoot, S. Hill, H. Xu, NOx control through reburning, Progress in energy and combustion science 24 (1998) 385–408.